



Bioactive glass 58S prepared using an innovation sol-gel process

Xuan Vuong Bui^{1,2,*}, Tan Hiep Dang³

¹Department for Management of Science and Technology Development, Ton Duc Thang University, Ho Chi Minh City, Vietnam

²Faculty of Applied Sciences, Ton Duc Thang University, Ho Chi Minh City, Vietnam

³Faculty of Chemical Engineering, Ho Chi Minh City University of Food Industry, Vietnam

Received 21 August 2018; Received in revised form 17 December 2018; Accepted 6 March 2019

Abstract

A 58S bioglass with a composition in the ternary system $58\text{SiO}_2\text{-}33\text{CaO-}9\text{P}_2\text{O}_5$ (wt.%) was prepared by an innovation sol-gel process in which a small amount of ammonia was used to facilitate the condensation reactions within an acidic solution prepared by tetraethyl orthosilicate, triethyl phosphate and calcium nitrate tetrahydrate. The properties of synthetic glass were investigated by several techniques. The amorphous nature and high specific surface area ($99.1\text{ m}^2/\text{g}$) of the obtained glass were confirmed by using X-ray diffraction and low-temperature nitrogen adsorption techniques, respectively. *In vitro* experiments were performed by soaking glass samples in the simulated body fluid (SBF). The XRD patterns and SEM images confirmed the bioactivity of the synthesized bioglass by formation of a dense and visible hydroxyapatite layer on its surface after 2 days of *in vitro* assays. The ICP-OES data illustrated the ion exchange behaviours between the bioglass 58S and the SBF solution.

Keywords: bioactive glass, sol-gel, freeze-drying, SBF, bioactivity, hydroxyapatite

I. Introduction

Bioactive glasses are a group of surface reactive biomaterials used as implants in the human body to repair and replace diseased or damaged bones because of their bioactivity [1–5]. Hydroxyapatite surface layer is formed when bioglasses are implanted in human body or soaked in simulated body fluid (SBF) solution. The composition of hydroxyapatite is similar to that of natural bone, so it allows bone grafting [1,3,6]. According to the published literature, the bioactivity mechanism of bioglasses was demonstrated by several steps [1,4,7,8]: i) rapid exchange of Na^+ , Ca^{2+} ions from glass network with H_3O^+ ions in physiological solution, ii) loss of silicic acid $\text{Si}(\text{OH})_4$ by breakage of Si–O–Si bridging links followed by formation of surface silanol groups, iii) condensation of SiO_2 rich surface layer by re-polymerisation of silanol groups, iv) an amorphous phosphorous-calcium rich layer is formed by migration of Ca^{2+} and PO_4^{3-} ions through the silica-rich layer, followed by thickening of this layer by incorporation of soluble Ca^{2+} and PO_4^{3-} ions from the SBF solution,

v) then, the amorphous layer of calcium phosphate is transformed into crystallizes by the OH^- , CO_3^{2-} ions incorporation.

Traditionally, bioactive glasses are prepared by melting process, in which the precursor materials are melted at high temperature. The first melting bioactive glass 45S5 containing 45 wt.% of SiO_2 , 24.5 wt.% of CaO , 24.5 wt.% of Na_2O and 6 wt.% of P_2O_5 was invented by Hench *et al.* [1]. This glass can chemically bind to host tissue by forming a bone-like apatite layer between artificial material and natural bone. Consequently, several studies on synthesis, *in vitro* and/or *in vivo* experiments of bioactive glasses, have been done by using theory of Hench [2,3,6,7].

Generally, the melting technique possesses some advantages such as fast production. However, this method contains some disadvantages such as: i) the volatile component of phosphate in the case of bioactive glasses containing P_2O_5 tends to evaporate at high temperature, ii) low value of specific surface area - an important factor to accelerate the deposition process of hydroxyapatite layer on the glassy surface after *in vitro* or *in vivo* experiments [4,9].

Recently, sol-gel method has been widely used to pre-

*Corresponding author: tel: +84 28 37755037, e-mail: buixuanvuong@tdtu.edu.vn

pare new bioactive glasses. Typically, common precursors for silica-based sol-gel glasses include alkoxides such as tetraethyl orthosilicate (TEOS), triethyl phosphate (TEP) or phosphoric acid, and salts of calcium as sources of SiO₂, P₂O₅, and CaO, respectively. Briefly, sol state is formed by hydrolysis, then, sol is transformed to gel by condensation process. The gelation is followed by ageing, drying, and thermal treatment at temperatures that typically vary in the range of 600–800 °C [10,11]. Main advantages of sol-gel technique are not only low reaction temperature between elements, but also highly homogeneous composition of particles of the obtained glass powder compared to that of the melting method. Furthermore, sol-gel method can be used for preparation of bioglasses with high specific surface area, being one of the key factors to promote the interactions between the bioglasses and the physiological environment, which causes the rapid formation of the biological apatite layer [9,11]. However, the sol-gel method usually requires several days for transition from sol to gel state [10,11].

In this study, the bioactive glass 58S with composition of 58SiO₂-33CaO-9P₂O₅ (wt.%) was synthesized using an innovation sol-gel process. Only a small amount of ammonia solution was used as an agent to stimulate the gelation and freeze-drying technique was used to dry the wet gel. The physico-chemical characterizations of the synthetic bioglass before and after *in vitro* experiments were investigated by different techniques.

II. Experimental procedure

2.1. Elaboration of 58S bioactive glass

The main precursors used in the sol-gel process were tetraethyl orthosilicate (TEOS, Si(OC₂H₅)₄, 99.999% purity, Sigma-Aldrich), triethyl phosphate (TEP, OP(OC₂H₅)₃, 99.8% purity, Sigma-Aldrich) and calcium nitrate tetrahydrate (Ca(NO₃)₂ · 4 H₂O, 99% purity, Sigma-Aldrich). First, 4.03 g of TEOS and 0.47 g of TEP were dissolved in 12 ml of distilled water. Three droplets of 2 M nitric acid were added to hydrolyse the precursors and to adjust pH at 1.1. After stirring for 0.5 h at room temperature, 2.81 g of calcium nitrate tetrahydrate was added and stirred at the same time as the step 1. The obtained mixture was a uniform, clear sol with the pH of 0.45. Next, three droplets of ammonia solution (30 wt.%, FlukaTM, pH = 13.3) were added into the sol to facilitate the condensation reactions of the sol to form the gel. Immediately after dropping the ammonia pH was changed to 7.2 and some gel granules were precipitated and the resulting mixture was continuously stirred for 1 h to completely form the condensed gel. In the previous studies [11,12], the exact amount of ammonia solution was used to set up the alkaline pH medium and condense the gel. In this research, a small amount of ammonia solution was used to produce some first gel particles. After that, the newly created gel particles acted as condensation nuclei seeds and stimulated

the gel formation in the whole reaction mixture. To remove excess water and ethanol from the wet gel, freeze-drying technique was used during 6 h. By using the ammonia solution as a gelation stimulating agent and the freeze-drying technique for gel drying the whole time for synthesis was shortened to about 10 h instead of a few days. The sample was solidified with liquid nitrogen and then lyophilized at temperature of –60 °C and vapour pressure of 0.01 mbar. Finally, the dried gel was converted into the bioactive glass 58S powder by treatment at 700 °C for 2 h. The resulting bioglass was pulverized in a mortar and sieved to achieve the particle sizes smaller than 80 μm, which were used for all characterizations.

2.2. *In vitro* test

The *in vitro* tests were undertaken to immerse the powder samples of bioactive glass in a container filled with the SBF. The composition of the SBF solution is similar to that of human blood plasma. It was prepared by using the Kokubo's method [13]. The samples were immersed in the SBF solution for 2, 5, 10 and 15 days and remained in an incubator at 37 °C. The ratio of glass powder to the solution volume of the SBF was 1 : 2 (100 mg/200 ml). After each time period, the samples were removed from the solution, gently rinsed three times with distilled water and dried for 1 day at room temperature.

2.3. Characterisation

The bioactive glass 58S before and after immersion in SBF solution was investigated by using several physico-chemical techniques. The specific surface area was determined by the low-temperature nitrogen adsorption-desorption measurements on multi-point BET, ASAP 2010 Analyzer. In order to identify the phase composition of synthetic bioactive glass and evaluate the formation of apatite layer after *in vitro* assay, X-ray diffraction (XRD) measurements were realised on Bruker D8 Advance diffractometer. Powder samples were mixed homogeneously with cyclohexane, dropped on the surfaces of plastic tablets and finally dried to remove the solvent. The XRD data were acquired with a scanning speed of 1°/min. The Fourier transformed infrared spectroscopy (FTIR) (Bruker Equinox 55) was employed to identify the functional groups of the bioactive glass before and after *in vitro* assay. Powder materials were ground and mixed thoroughly with KBr powder in the ratio 1 : 100. FTIR spectra were recorded in the wave number range of 400 and 4000 cm⁻¹, at a resolution of 2 cm⁻¹. Scanning electron microscopy (SEM, JEOL JSM 6301) was used to evaluate the morphological surface of bioactive glass as a function of soaking time in SBF. In addition, the pH and ion concentration behaviour of the SBF solution during the *in vitro* experiments were also monitored by using the pH meter and Inductively coupled plasma optical emission spectrometry (ICP-OES) technique.

III. Results and discussion

Figure 1 shows the XRD diagrams of the bioactive glass 58S before and after soaking in SBF solution for different time periods. The XRD diagram of the pure hydroxyapatite purchased from the Sigma-Aldrich is presented as a reference to estimate the bioactivity of the bioactive glass as a function of immersion time in the *in vitro* experiments. Before immersion, the sample was amorphous showing glassy nature (Fig. 1a). However, hydroxyapatite (HA) phase has been formed after immersion of bioactive glass powder in the SBF for 2 days (Fig. 1b) [14] confirmed by appearance of two characteristic HA peaks at 26° (002) and 32° (211). Other less obvious peaks could also be seen at 40° (310), 46.7° (222), 50° (213) and 53° (004). The above observation confirmed the bioactivity of the synthetic bioactive glass. The peaks of the HA phase have become sharper when the soaking time increased, which was assigned to further transformation of the bioactive glass to HA (Figs. 1c,d).

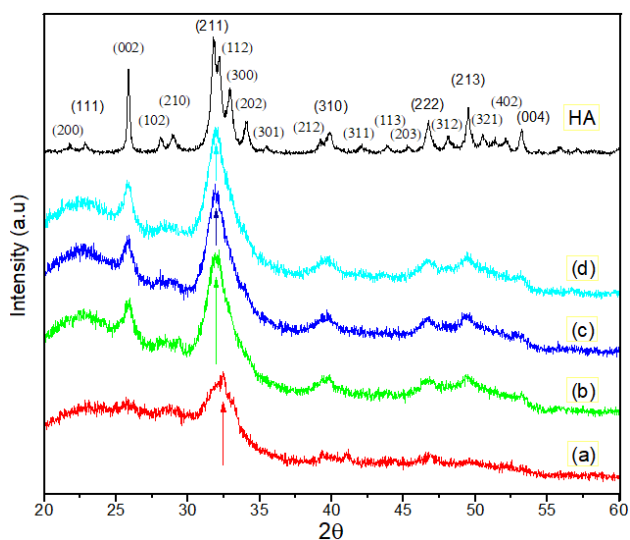


Figure 1. XRD patterns of bioactive glass 58S before (a) and after soaking in the SBF for: (b) 2, (c) 5 and (d) 10 days

FTIR spectra of the bioactive glass 58S before and after soaking in SBF solution are presented in Fig. 2. According to the references, the synthetic bioactive glass 58S indicated the majority of characteristic bands of silica network (Fig. 2a). The bands at 470 , 800 and 1100 cm^{-1} were attributed to the deformation vibration of Si–O–Si bridging bonds in the SiO_4 tetrahedrons which have four oxygen atoms linked to four Si neighbours; these tetrahedrons are noted as $\text{Q}^4(\text{Si})$ [15]. The bands at 870 , 950 and 1040 cm^{-1} correspond to the stretching vibration of Si–O–Si bonds in the $\text{Q}^1(\text{Si})$, $\text{Q}^2(\text{Si})$ and $\text{Q}^3(\text{Si})$ tetrahedrons, respectively, which include 1, 2 and 3 bridging oxygen atoms [16]. The band at 1230 cm^{-1} relates to the symmetric and anti-symmetric modes of Si–O–Ca bonds in the $\text{Q}^0(\text{Si})$ units which have non-bridging oxygen atoms [17]. In addition, two bands at 570 and 605 cm^{-1} were characteris-

tic of bending vibration of P–O liaisons in the PO_4^{3-} groups which correspond to the tetrahedron $\text{Q}^0(\text{P})$ or $\text{Q}^1(\text{P})$ [18]. Their intensity was weak due to the small amount of phosphate linked to the glassy matrix [19,20]. After immersing in the SBF solution (Figs. 2b,c,d), the bands characteristic for Si–O liaisons at 470 and 800 cm^{-1} became more visible. This confirmed the formation of SiO_2 rich surface layer due to the dissolution of the glassy network [1,7]. Especially, two P–O characteristic bands were moved to the right. They clearly appeared at 560 and 600 cm^{-1} . These bands were attributed to the stretching vibrations of PO_4^{3-} group in the crystalline phase of the hydroxyapatite material [19,20]. This result combined with the XRD analysis confirmed the bioactivity of the synthetic bioactive glass 58S.

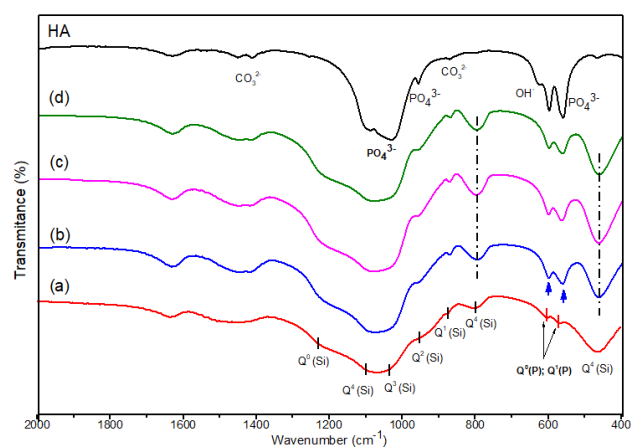


Figure 2. FTIR spectra of bioactive glass 58S before (a) and after *in vitro* experiments for: (b) 2, (c) 5 and (d) 10 days

SEM surface images of the bioactive glass 58S following the immersion times are presented in Fig. 3. The synthetic bioactive glass 58S showed the rough surface and porous structure. After soaking in the SBF solution, the surface structure of the bioactive glass 58S changed as a result of the interfacial chemical reactions between the glass powder and the physiological solution. The surface of glass was completely covered with small, visible and homogeneous particles after 2 days of soaking in the SBF solution (Fig. 3b). With the increase in soaking times, the particles became bigger and clearer (Figs. 3c,d) due to the gradual crystallization of HA on the bio-glass surface. The specific surface area of the obtained bioactive glass 58S is $99.1\text{ m}^2/\text{g}$. This value is similar to that of bioactive glass 58S synthesized by convention sol-gel method and much higher than that of 45S melted bioactive glass [9,21]. Thus, the 58S bioglass with the grain size in a range of $32\text{--}63\text{ }\mu\text{m}$ has the specific surface area of $95\text{ m}^2/\text{g}$ [9], and the 45S bioglasses with grain sizes in the range of $5\text{--}20$, $90\text{--}300$ and $90\text{--}710\text{ }\mu\text{m}$ have the specific surface areas of 2.7 , 0.24 and $0.15\text{ m}^2/\text{g}$, respectively.

The pH change of the SBF solution with time is shown in Fig. 4. The initial pH of SBF was 7.4 . From 2 to 10 days, the pH of the SBF solution increased from

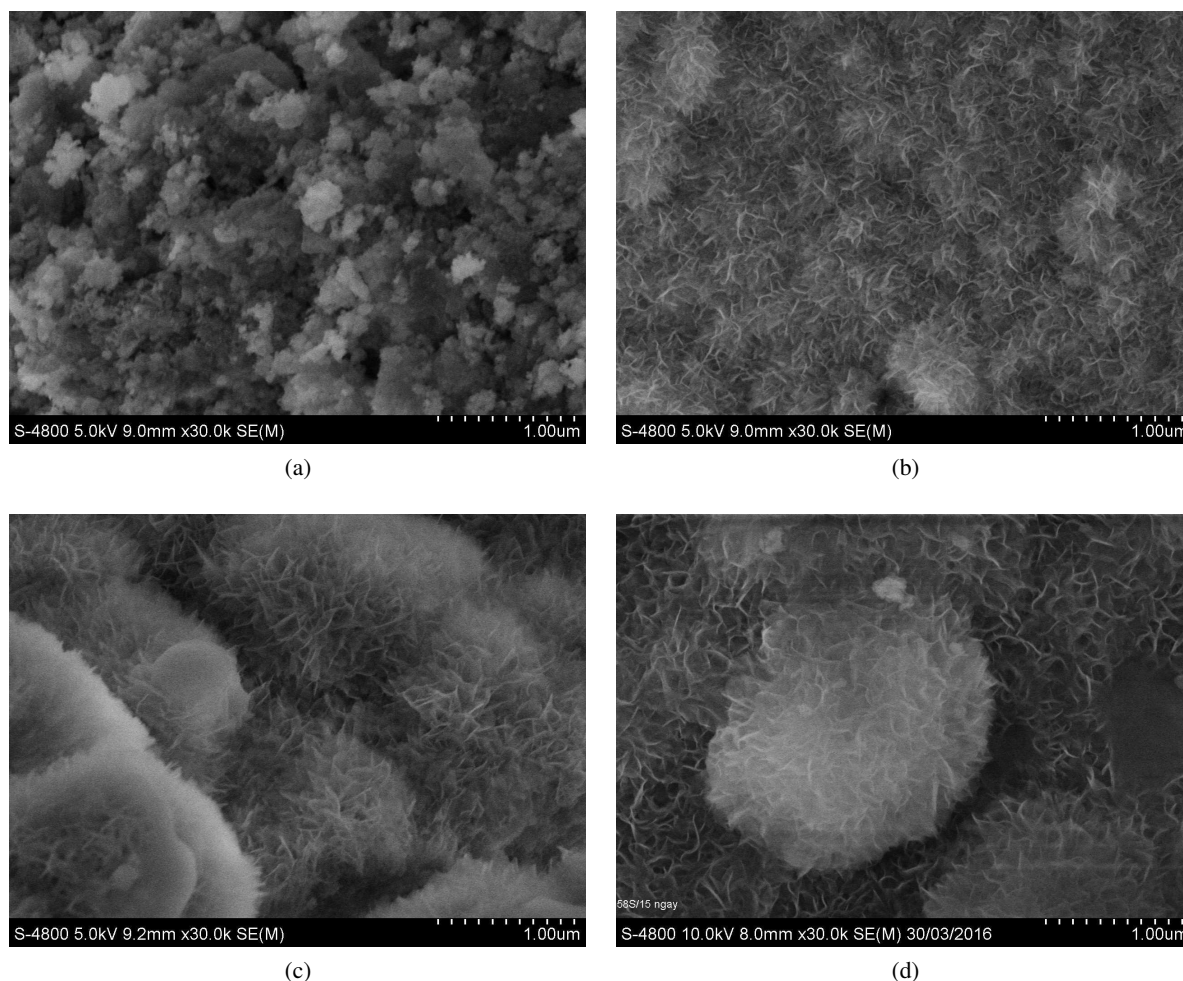


Figure 3. SEM images of bioactive glass 58S before (a) and after *in vitro* experiments: b) 2, c) 5 and d) 10 days

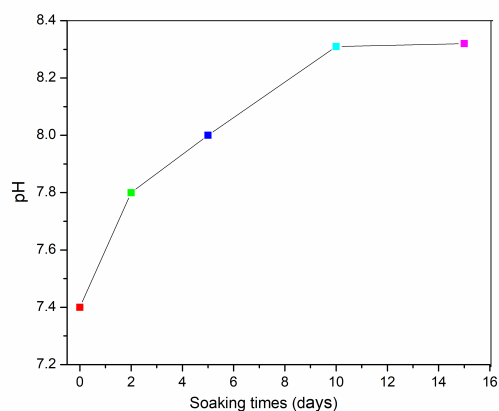


Figure 4. Change of pH value of the SBF solution during the *in vitro* test

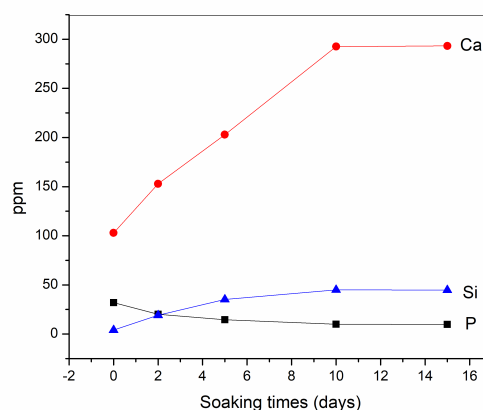


Figure 5. Ca, Si, P concentration behaviours of the SBF during the *in vitro* test

7.8 to 8.3, whereas the change of pH value was not significant after 10 days.

Figure 5 shows the variations of silicon, calcium and phosphorus concentrations in the SBF solution as a function of soaking time, measured by the ICP-OES method. According to the references, the changes of ionic concentrations in the SBF solution are related to

the dissolution of glassy network and the precipitation of HA layer [7,11]. The initial SBF liquid did not contain silicon. In the SBF liquid silicon ions can appear due to the loss of the soluble $\text{Si}(\text{OH})_4$ by breaking Si–O–Si bonds under the interactions of the glassy network with the SBF liquid. After 15 days of soaking, the concentration of Si ions increased from 0 to 41 ppm. During

the first five days of soaking in the SBF solution, the Si concentration increased strongly from 0 to 31.2 ppm. In the second period (from 5 to 10 days) the silicon concentration increased moderately before reaching the stable level (from 10 to 15 days). The appearance of Ca and P ions in the SBF solution is related to two opposite processes: the release of Ca and P from the glass network results in the increase of their concentration in the SBF; the consumption of Ca and P during the formation of apatite layer causes the decrease of their concentration [7,11]. The Ca concentration jumped from 100.9 ppm (0 day) to 290.56 ppm (10 days) and then it was stabilized. The XRD results confirmed that the hydroxyapatite layer has formed on the bioglass' surface after only 2 days. Thus, the change of Ca concentration (Fig. 5) indicates that the release of Ca ions is higher than their consumption in the first 10 days. For the period of 10 to 15 days, it is obvious that the release of Ca and the consumption of Ca was balanced which reached a stable period as observed in the Fig. 5. This result is perfectly consistent with the pH analysis (Fig. 4) because the Ca concentration in the SBF liquid is proportional to pH. The change in P concentration showed a difference in comparison to Ca. The P concentration in the initial SBF solution was 31.2 ppm. No increase in P concentration in the SBF solution was observed. This highlighted that the P consumption for apatite layer formation is higher than the P release from the glass network. This result can be explained by the low P content in the 58SiO₂-33CaO-9P₂O₅ glass system. Furthermore, the P element is the network former existing in the covalently bond –O–Si–O–P– while the Ca element as network modifier is present in the ionic bond –O–Si–O–Ca²⁺–O–P– [22]. The disruption of covalent bonds in –O–Si–O–P– may be more difficult than the rapid ion exchange of network modifying Ca²⁺ ions with H₃O⁺ ions in the SBF fluid. This can cause the release of low amount of P. It is clear from the above results that the interaction between the SBF and the glass samples occurs during *in vitro* time, including: i) the dissolution of glass network, ii) release of Ca, P and iii) incorporation of Ca and P in the formed apatite layer on the glass' surface.

IV. Conclusions

The bioactive glass 58S has been successfully prepared by an innovative sol-gel process. In this way, a fast process for transformation from the sol to the gel was done by adding ammonia solution and then, the gel was dried by using the freeze-drying technique for 6 hours. The bioactive glass 58S shows glassy characteristic and high specific surface area (99.1 m²/g). The *in vitro* assay was carried out by soaking glass samples in SBF solution for different times. The obtained results highlighted the bioactivity of synthetic bioglass through the formation of a dense and visible apatite layer on its surface after 2 days of *in vitro* experiment.

Acknowledgement: The authors would like to ac-

knowledge Thi Hoa Bui, Chonnam University, Korea for scientific discussion.

References

1. L.L. Hench, "The story of Bioglass", *J. Mater. Sci. Mater. Med.*, **17** [11] (2006) 967–978.
2. E. Wers, H. Oudadesse, B. Lefeuvre, B. Bureau, O. Merdrignac-Conanec, "Thermal investigations of Ti and Ag-doped bioactive glasses", *Therm. Acta.*, **580** (2014) 79–84.
3. H. Oudadesse, E. Dietrich, Y.L. Gal, P. Pellen, B. Bureau, A.A. Mostafa, G. Cathelineau, "Apatite forming ability and cytocompatibility of pure and Zn-doped bioactive glasses", *Biomed. Mater.*, **6** [3] (2011) 35–44.
4. J.R. Jones, "Review of bioactive glass: From Hench to hybrids", *Acta. Biomater.*, **9** [1] (2013) 4457–4486.
5. M.N. Rahaman, D.E. Day, B.S. Bal, Q. Fu, S.B. Jung, L.F. Bonewald, A.P. Tomsia, "Bioactive glass in tissue engineering", *Acta. Biomater.*, **7** [6] (2011) 2355–2373.
6. H. Oudadesse, E. Dietrich, X.V. Bui, Y.L. Gal, P. Pellen, G. Cathelineau, "Enhancement of cells proliferation and control of bioactivity of strontium doped glass", *Appl. Surf. Sci.*, **257** [20] (2011) 8587–8593.
7. E. Dietrich, H. Oudadesse, A. Lucas-Girot, Y.L. Gal, S. Jeanne, G. Cathelineau, "Effects of Mg and Zn on the surface of doped melt-derived glass for biomaterials applications", *Appl. Surf. Sci.*, **255** [2] (2008) 391–395.
8. L.L. Hench, R.J. Splinter, W.C. Allen, T.K. Greenlee, "Bonding mechanisms at the interface of ceramic prosthetic materials", *J. Biomed. Mater. Res.*, **5** [6] (1971) 117–141.
9. S. Sepulveda, J.R. Jones, L.L. Hench, "Characterization of melt-derived 45S5 and sol-gel-derived 58S bioactive glasses", *J. Biomed. Mater. Res.*, **58** [6] (2001) 734–740.
10. G.J. Owens, R.K. Singh, F. Foroutan, M. Alqaysi, C.M. Han, C. Mahapatra, H.W. Kim, J.C. Knowles, "Sol-gel based materials for biomedical applications", *Prog. Mater. Sci.*, **77** (2016) 1–79.
11. N. Letaïef, A. Lucas-Girot, H. Oudadesse, P. Meleard, T. Pott, J. Jelassi, R. Dorbez-Sridi, "Effect of aging temperature on the structure, pore morphology and bioactivity of new sol-gel synthesized bioglass", *J. Non. Cryst. Sol.*, **402** [15] (2014) 194–199.
12. W. Xia, J. Chang, "Preparation and characterization of nano-bioactive-glasses (NGB) by a quick alkali-mediated sol-gel method", *Mater. Lett.*, **61** (2007) 3251–3253.
13. T. Kokubo, H. Takadama, "How useful is SBF in predicting *in vivo* bone bioactivity", *Biomaterials*, **27** [15] (2006) 2907–2915.
14. X.V. Bui, H. Oudadesse, Y.L. Gal, O. Merdrignac-Conanee, G. Cathelineau, "Bioactivity behaviour of biodegradable material comprising bioactive glass", *Korean. J. Chem. Eng.*, **29** [2] (2012) 215–220.
15. P. Innocenzi, "Infrared spectroscopy of sol-gel derived silica-based films: a spectra-microstructure overview", *J. Non-Cryst. Solids*, **316** (2003) 309–319.
16. C.I. Merzbacher, W.B. White, "Structure of Na in aluminosilicate glasses - a far-infrared reflectance spectroscopic study", *Am. Mineral.*, **73** (1988) 1089–1094.
17. A.G. Kalampounias, "IR and Raman spectroscopic studies of sol-gel derived alkaline-earth silicate glasses", *Bull. Mater. Sci.*, **34** (2011) 299–303.
18. J. Ding, Y. Chen, W. Chen, L. Hu, G. Boulon, "Effect of

- P₂O₅ addition on the structural and spectroscopic properties of sodium aluminosilicate glass”, *Chin. Opt. Lett.*, **10** [7] (2012) 071602.
19. T.S. Huang, M.N. Rahaman, N.D. Doiphode, M.C. Leu, B.S. Bal, D.E. Day, X. Liu, “Porous and strong bioactive glass (13-93) scaffolds fabricated by freeze extrusion technique”, *Mater. Sci. Eng. C*, **31** [7] (2001) 1482–1489.
 20. M. Handke, M. Sitarz, M. Rokita, E. Galuskin, “Vibrational spectra of phosphate-silicate biomaterials”, *J. Mol. Struct.*, **651** (2003) 39–54.
 21. M.V. Regi, C.V. Ragel, A.J. Salinas, “Glasses with medical applications”, *Eur. J. Inorg. Chem.*, **6** (2003) 1029–1042.
 22. M.V. Regi, “Ceramics for medical applications”, *J. Chem. Soc. Dalton. Trans.*, **2** (2001) 97–108.